# The Kinetics and Mechanism of Water Evolution from Molten dl Lithium Potassium Tartrate Monohydrate

Sreelekha D. Bhattamisra, Genevieve M. Laverty, Nikolai A. Baranov, Vladimir B. Okhotnikov and Andrew K. Galwey

*Phil. Trans. R. Soc. Lond. A* 1992 **341**, 479-498
doi: 10.1098/rsta.1992.0112

# The kinetics and mechanism of water evolution from molten *dl* lithium potassium tartrate monohydrate

By Sreelekha D. Bhattamisra†, Genevieve M. Laverty,
Nikolai A. Baranov‡, Vladimir B. Okhotnikov‡
and Andrew K. Galwey

*School of Chemistry, The Queen's University of Belfast, Belfast BT9 5AG, U.K.*

A kinetic and microscopic investigation of the thermal dehydration of *dl* lithium potassium tartrate monohydrate is reported and the reaction mechanism discussed. This work forms part of a more comprehensive study concerned with the influence of reactant structure on the reactivity and the mechanism of chemical change. The other hydrated reactants with which this salt will be compared contain the *d* and *meso* forms of the tartrate anion and crystallize with different structures.

*dl* lithium potassium tartrate monohydrate lost the single molecule of water of crystallization in one predominantly deceleratory process that was studied between 350–460 K. Reaction was accompanied by melting to yield a residual glassy anhydrous product that was amorphous to X-ray diffraction. An initial, relatively rapid release of water (6%) was followed by a deceleratory process that led to a zero-order reaction (that, in crystals, extended between 18% and 80%) before completion by an approximately first-order stage. Dehydrations of crushed powder reactant samples differed from single crystals in being relatively more rapid (an eight-fold increase); the deceleratory process was long and the zero-order process shorter (50–85%). The activation energy for dehydrations of crystal and of powder was $330 \pm 30$ kJ $\text{mol}^{-1}$.

This pattern of kinetic behaviour was not in accordance with expectation for a homogeneous reaction, the rate was not directly related to reactant concentration terms. Alternative analyses of the obedience of data to rate expressions applicable to solid state reactions were equally unsuccessful. Our mechanistic interpretation of the rate data, therefore, considered *a priori* the factors expected to participate in the control of water evolution from the melt. It is concluded that the vitreous or molten phase is not homogeneous and, therefore, behaviour is different from reactions in an isotropic fluid or in a solid. Two models are proposed to explain our observations. In the *two phase equilibrium* mechanism it is assumed that the reactant particles are composed of two phases, zones of hydrate are embedded in dehydrated material that retains a constant but small proportion of water. (These phases participate in an equilibrium analogous to that of liquid/vapour.) The *surface boundary layer* model

---

† Permanent address: Department of Chemistry, Berhampur University, Berhampur 760007, India.

‡ Permanent address: Institute of Solid State Chemistry, Academy of Sciences, Siberian Branch, Derzhavina 18, 630091, Novosibirsk, Siberia.

*Phil. Trans. R. Soc. Lond.* A (1992) **341**, 479–498
*Printed in Great Britain*

envisages the initial development of a peripheral barrier zone through which the constant rate of water diffusion is rate controlling.

This class of reaction, proceeding in a fluid but the absence of added solvent, has received relatively little attention. The present discussion is intended to identify the characteristic behaviour and draw attention to the necessity to consider such mechanisms in discussions of reactions of solids where there is the possibility of melt participation.

## 1. Introduction

Kinetic and microscopic investigations of dehydrations have contributed very significantly to the development of the theory of solid state reactions (Brown *et al.* 1980). Crystalline hydrates have often been selected as reactants used in studies to characterize the role of the reactant/product contact interface during chemical change (Garner 1955). Some reactions of this type exhibit nucleation and growth behaviour and consideration of the systematic development of an advancing interface has yielded a set of rate equations that are widely applied in kinetic measurements of dehydrations, thermal decompositions and other reactions of solids (Brown *et al.* 1980). Interest in dehydrations continues, however, often specifically concerned with identifying the chemical steps that result in interface advance (Galwey & Laverty 1990).

This paper reports a detailed kinetic and mechanistic study of the dehydration of *dl* lithium potassium tartrate monohydrate. This work is part of a more comprehensive programme undertaken to compare reactivities in a group of exceptionally closely related reactants. Recently we (Baranov *et al.* 1990) pointed out that hydrated lithium potassium tartrates containing the *d*, the *dl* and the *meso* stereochemical forms of the anion crystallize with different structures and are dehydrated in different temperature intervals to give products of different crystalline order. Accordingly, we recognize this group of hydrates, consisting of identical chemical constituents bonded in different spatial dispositions, as providing a set of reactants that are particularly suitable for investigation of the effects of structure on reactivity. Structures of these solids have not been established but it is reasonable to assume that the water of crystallization is retained by the extensive possibilities for hydrogen bonding with the anion.

Detailed kinetic and microscopic studies of the dehydrations of both the *dl* salt monohydrate and the *d* salt monohydrate have already been completed in our laboratories. It is appropriate to introduce the work here by giving brief descriptions of the different patterns of behaviour shown. This paper is concerned with *dl* $LiKC_4H_4O_6 . H_2O$. In Laverty *et al.* (1992), results of the *d* salt will be presented, together with useful comparisons with the observations reported here.

Water losses during the dehydration of *d* lithium potassium tartrate monohydrate proceeds to completion through two distinct rate processes (Laverty *et al.* 1992). The first reaction is the diffusion controlled (Galwey & Okhotnikov 1988) release of water from a disorganized surface layer, extending to a thickness *ca.* 10 μm. This deceleratory process is identified as occurring in a water site vacancy structure (Okhotnikov *et al.* 1987; Galwey & Okhotnikov 1988) that develops as reaction continues. The subsequent (second) reaction is a nucleation and growth process proceeding beneath the initially formed superficial dehydrated layer and through which the evolved water vapour escapes, characteristically involving bubble formation (Guarini & Rustici 1987).

In contrast, *dl* lithium potassium tartrate monohydrate melts during dehydration. The residue is amorphous to X-ray diffraction (Baranov *et al*. 1990), crystals adhered to the walls of the reaction vessel and powders sintered to form a single coherent reactant particle. This study is, therefore, novel and interesting because it is the dehydration of a molten reactant.

The kinetics of reactions proceeding in a melt, alternatively regarded as homogeneous reactions occurring in the absence of an added solvent, have not been extensively characterized. This paper reports and discusses the properties of this interesting but unfamiliar type of rate process. It is not possible to anticipate, with confidence, the pattern of kinetic behaviour for such processes because two alternative, but quite different forms of control may determine the overall rate of chemical change. Dehydration could proceed as a homogeneous process in which water release occurs throughout the reactant bulk and rate is controlled by concentration terms. Alternatively dehydration may occur exclusively at reactant particle boundaries, or at an interface, so that it is more appropriately considered to exhibit a formal similarity with solid state behaviour (Brown *et al*. 1980). Thus the characterization of the kinetic properties of a process involving a fused reactant is expected to be of value in contributing to mechanistic interpretations of other solid state reactions in which local or more extensive melt formation is often a possibility (Carr & Galwey 1986).

Kinetic observations for the dehydration of *dl* lithium potassium tartrate monohydrate are reported and discussed below in the context of the alternative homogeneous and heterogeneous reaction mechanisms. We are aware of no previous study for this reactant except the preliminary observations by Baranov *et al*. (1990).

## 2. Experimental

### (*a*) *Reactant salt*

The racemic salt, *dl* lithium potassium tartrate monohydrate, was crystallized by solvent evaporation at 373 K from an aqueous solution containing the appropriate stoichiometric amounts of LiOH, KOH and *dl* tartaric acid. The crystallites were removed by filtration and dried in air at ambient temperature. The preparations investigated were shown by combustion analyses (C, 22.34 % and 22.12 %; H, 2.78 % and 2.63 %) and weight loss determinations to be in accordance with expectation for *dl* $LiKC_4H_4O_6.H_2O$ (C, 22.65 %; H, 2.85 %).

### (*b*) *Kinetic studies: water evolution measurements*

The experimental technique used to measure reaction rates was identical to that described previously (Carr & Galwey 1985). The reactant sample, contained in a small glass tube and placed in the glass apparatus, was evacuated to less than 1 N $m^{-2}$ before being isolated from the pumps and admitted to the constant temperature (±0.5 K) reaction zone. Reactant temperature was measured by a thermocouple positioned as closely as possible outside the vacuum envelope. The reactant sample attained the controlled reaction temperature within 5 min of admission to the heated zone. Water evolved was determined from the pressure rise in the constant volume apparatus, measured by an MKS 222B absolute pressure gauge, working in the range 0–1500 N $m^{-2}$ and read with an accuracy of 0.1 N $m^{-2}$. This gauge was interfaced with a computer that stores (time, pressure and temperature) data at preselected time intervals, subject to the condition that a specified pressure rise has occurred since the previously recorded value. Reading frequency is, therefore, related to reaction rate.

Computer programs enable recorded pressure values to be calculated as fractional reaction ($\alpha$) based on the completed water evolution from the monohydrate. Facilities were also available for testing obedience of the $\alpha$-time data for the isothermal dehydration to those kinetic expressions that are characteristic of reactions of solids (Brown *et al.* 1980).

### (*c*) *Kinetic studies: weight loss measurements*

The kinetics of dehydration during the initial stages of reaction were measured using a quartz crystal microbalance (Okhotnikov & Lyakhov 1984). The single crystal reactant specimen, in the form of a disc, 3 mm radius and 1 mm thickness, was held at constant temperature $\pm 0.1$ K and weight changes were measured with accuracy $\pm 10^{-8}$ g. A dynamic vacuum $7 \times 10^{-5}$ Pa was maintained throughout each experiment over the single face from which water loss occurred: other surfaces were rendered inactive by a covering of indium–gallium eutectic (Galwey & Okhotnikov 1988).

### (*d*) *Electron microscopy*

Samples of the prepared monohydrate, the anhydrous product and specimens of salt partially dehydrated to known extents ($\alpha \pm 0.01$) were examined in a Jeol 35CF scanning electron microscope to characterize surface features. Internal structures were revealed by fracture sections of individual particles exposed by gentle crushing after reaction. Each sample was rendered conducting by a thin coating of Au/Pd before being placed in the microscope. Low electron accelerating voltages were used throughout to minimize beam damage to the specimen.

## 3. Results and discussion

### (*a*) *Electron microscopy*

We present the electron microscopic observations before the rate studies, to enable the kinetic data to be interpreted with due consideration of the textural changes that occur during dehydration. A knowledge of the physical structure and texture of the reactant can be most valuable in the formulation of a reaction mechanism. The present conclusion that during dehydration the salt melts was an essential consideration for the interpretation of the rate characteristics.

Observations, visual and using the optical microscope, showed that particles of the partly dehydrated salt exhibited rounded features attributed to control by surface free energy rather than by crystallographic forces. Glass fibres often adhered to, or were embedded in, the surfaces of the dehydrated particles. Crushed crystal reactant samples sintered during dehydration to form coherent aggregates that hardened on cooling and within which there were bubbles and channels; again, the ubiquitous occurrence of rounded surfaces indicated particle shape control by surface free energy. Such aggregates adhered to the glass wall of the containing vessel. There was no evidence of the generation of locally textured zones that could be recognized as

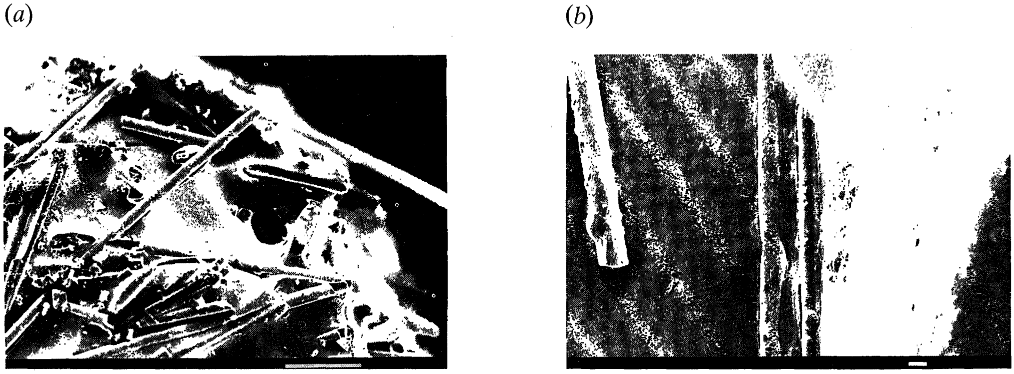

Figure 1. External surface of a partly dehydrated crystal of *dl* lithium potassium tartrate monohydrate ($\alpha = 0.33$ at 450 K). Reactant melting is demonstrated by the wetting of glass wool fibres which are retained, embedded in the residue, which hardened on cooling. (Scale bars: (*a*) 100 μm; (*b*) 10 μm.)

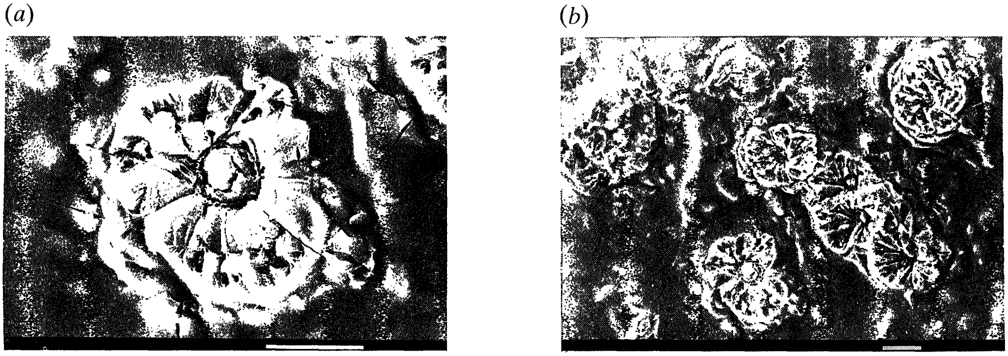

Figure 2. Characteristic surface textural features found on surfaces of partially dehydrated crystals ($\alpha = 0.43$ at 453 K). These features are identified as sites of collapsed bubbles acting as vent holes for the escape of steam from intracrystalline pores within which the volatilized water is temporarily retained. (Scale bars: both 10 μm.)

nuclei. These observations lead us to conclude that dehydration is accompanied by at least partial and possibly comprehensive fusion of the reactant. This conclusion is entirely supported by the scanning electron microscope observations that are presented in detail below.

### (i) *Single crystal reactant*

During the dehydration of single crystals of *dl* lithium potassium tartrate monohydrate, glass fibres, used to retain the crystal in the sample tube, penetrated the outer boundaries of the reactant mass. The appearance of wetting and the retention of such fibres embedded in the residual material after resolidification on cooling is evidence that the reactant melted to form a viscous liquid: representative electron micrograph illustrations to support this conclusion are given in figure 1*a*, *b* ($\alpha = 0.33$). Characteristic textural features found at the surfaces of partly dehydrated ($\alpha = 0.43$) salt are shown in figure 2*a*, *b*. These rounded structures are identified as scars remaining after the collapse of bubbles which are the sites of steam release from pockets after passage through the viscous (possibly vitreous) material to the outer

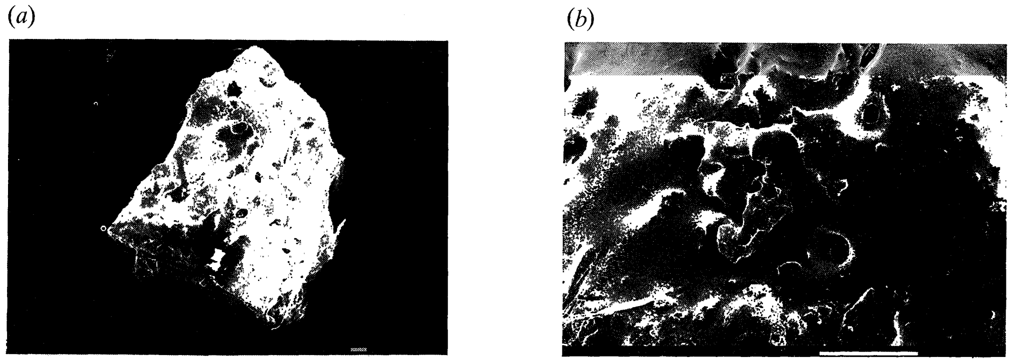

Figure 3. Surface texture of dehydrated salt ($\alpha = 1.00$ at 453 K); the flat surface characteristic of the original reactant crystals has been lost. The outer boundary faces of the crystal have become covered with rounded features, indicative of surface tension control operating in the molten reactant surface during water loss. (Scale bars both: 100 μm.)

Figure 4

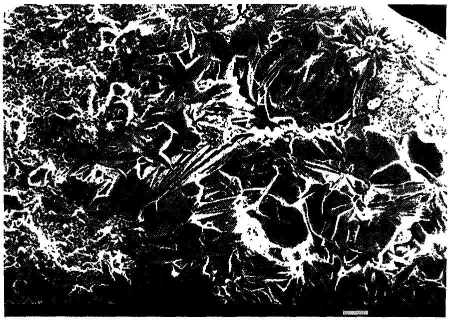

Figure 5

Figure 4. After limited dehydration ($\alpha = 0.1$ at 442 K) the surface of this crystal gives evidence of recrystallization on cooling. (Scale bar: 10 μm.)

Figure 5. This feature, unique in the present work, is interpreted as evidence of superficial melting in which the viscous boundary phase has been pulled outwards during temporary attachment to (perhaps) a glass fibre. (Scale bar: 10 μm.) ($\alpha = 0.33$ at 450 K.)

boundary layer of the reactant particle. Comparable textures are also seen in figure 1*b*.

Following completed dehydration ($\alpha = 1.00$), the originally planar surface characteristic of the prepared salt has become irregular due to the development of various sized protuberances and holes (figure 3*a*, *b*). In contrast, the surfaces of crystals that had undergone much less extensive water losses, e.g. $\alpha = 0.1$ in figure 4, appeared to have undergone recrystallization on cooling. The unusual feature in figure 5 ($\alpha = 0.33$) is presented as evidence of salt melting; this structure is most reasonably interpreted as a portion of viscous surface mechanically pulled outwards by temporary attachment, perhaps to a glass fibre.

Examination of surfaces exposed by fracture after partial ($\alpha = 0.5$) reaction showed appearances similar to those characteristic of a cleaved reactant crystal (figure 6*a*, *b*). Surfaces were flat and featureless between typical step edges. There was no evidence of any texture identifiable as a nucleus or areas of textural variations attributable to a nucleation and growth reaction. There were, however,

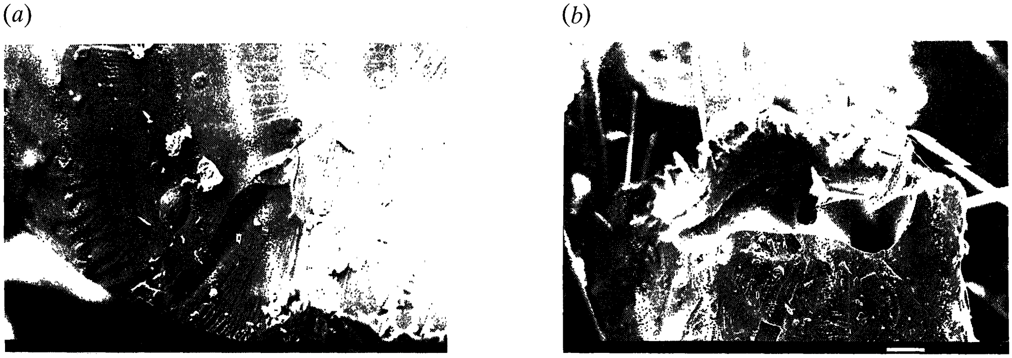

Figure 6. Sections of reactant crystal cleaved after partial dehydration, $\alpha = 0.50$ at 438 K. Some areas in (*a*) resembled the exposed faces of cleaved reactant crystals; there was no evidence of nucleus development and no features other than cleavage step edges were found. Other areas in (*b*) included large pores and retained embedded glass fibres. (Scale bars: (*a*) 10 μm; (*b*) 100 μm.)

Figure 7

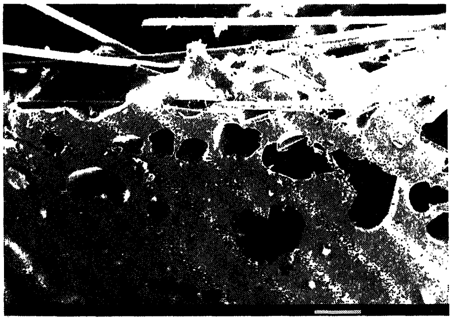

Figure 8

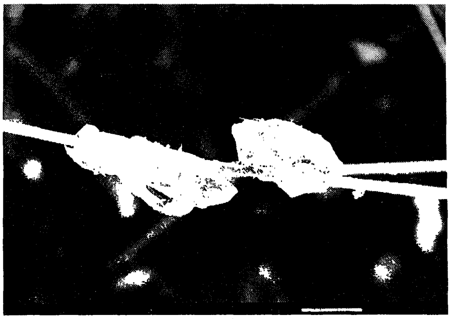

Figure 7. Aggregate large particle formed by sintering of powder sample after partial dehydration to $\alpha = 0.60$ at 437 K. The flat surface in the lower part of the photograph is material that adhered to the glass wall of the containing vessel and in the upper part the retention of embedded glass fibres is seen. (Scale bar: 100 μm.)

Figure 8. Same sample as figure 7, some small particles remain attached, following fusion, to glass wool fibres (used to retain sample in the reaction tube). (Scale bar: 100 μm.)

large intraparticulate cavities, probably zones of water accumulation before expulsion through bubble cavities that leave scars of the type seen in figure 2.

### (ii) *Crushed powder reactant*

The textures of the reactant matrix after onset of dehydration of crushed power reactant samples were closely similar to those of single crystal reactants except for the larger numbers of internal cavities within the comprehensively fused aggregates. The partly reacted sample ($\alpha = 0.6$) in figure 7 shows the hard, coherent reactant mass formed by the melting together of powder particles (1–10 μm edge). The lower half of the photograph shows the smooth surface of the compact aggregate that had fused and moulded to the glass container wall. Bubble formation is evidence of intraparticulate water retention. Again glass fibres, used to restrain the sample within the reactant glass vessel, have become embedded in the fused mass and some individual salt particles have adhered to fibres (figure 8).

Figure 9

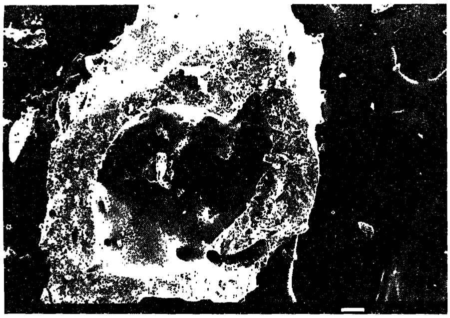

Figure 10

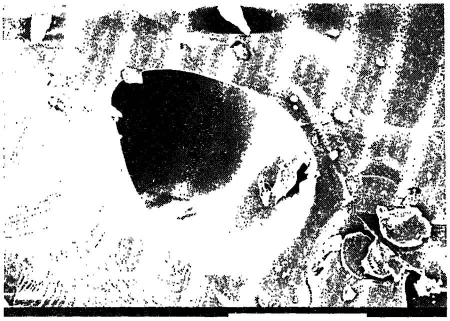

Figure 9. This aggregate was formed by the fusion of crushed powder reactant at $\alpha = 0.1$ (430 K). Fracture of the sample revealed the large central hole. (Scale bar: 100 μm.)

Figure 10. The cleavage surface of this aggregate formed by the sintering of a crushed powder sample ($\alpha = 0.60$ at 448 K) shows a large pore and coherent reactant phase in which no features or textural variations can be discerned. (Scale bar: 100 μm.)

Fusion of the reactant powder crystallites occurred rapidly after the initial onset of water loss, the coherent particle in figure 9 has formed at $\alpha = 0.1$ and contained a large bubble in the centre revealed on fracture. Another large pore is seen in figure 10 for salt dehydrated to $\alpha = 0.6$. Careful examination of the fracture faces in this and other similar photographs yielded no evidence of any characteristic texture that could be identified as a product phase or the development of zones which could be recognized as nuclei. Textures of outer surfaces again showed evidence of rounded protuberances and undulating surfaces (figure 11) while on other areas of the same sample, bubble escape scars were again found (figure 12).

### (iii) *Discussion*

Coalescence of the particles of powder reactant to form a single coherent aggregate, together with the wetting of glass fibres which are retained embedded in the material solidified on cooling, is clear evidence of fusion. Extensively or completely dehydrated salt showed no features that are characteristic of crystals, such as planar faces, orientation and alignment of features, etc. The rounded protuberances and hollows of dehydrated surfaces were entirely consistent with control by surface free energy rather than crystallographic forces.

Dehydration was accompanied by the development of intraparticulate holes, often large (see figures 6*b* and 7) and always bounded by rounded surfaces. These cavities are ascribed to internal water vapour accumulations, formally bearing similarities to the boiling process in liquids. Water vapour escape from such holes requires the penetration of the outer, relatively more extensively dehydrated surface zone and accounts for the rounded, 'collapsed bubble' features shown in figure 2.

Although sought, no evidence could be found of any alternative texture that could be recognized as an anhydrous product salt and no areas identifiable as growth nuclei were detected. The textures of all surfaces revealed by fracture after reaction were featureless, similar in appearance to cleaved, relatively perfect, reactant crystals. This is consistent with expectation for this salt in which the anion offers extensive possibilities for hydrogen bonding. At dehydration temperature the structure may be regarded as a highly viscous fluid, there is effectively comprehensive melting and loss

Figure 11

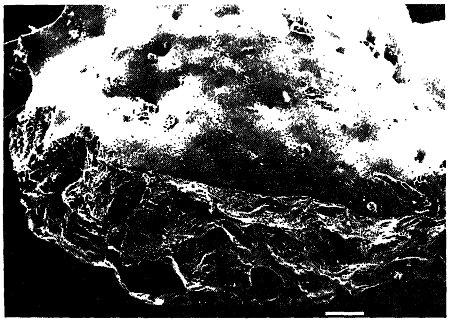

Figure 12

Figure 11. At an early stage in dehydration of a crushed powder reactant sample ($\alpha = 0.1$ at 430 K) the fused salt showed superficial rounded features indicative of control by surface tension rather than crystallographic forces. (Scale bar: 100 µm.)

Figure 12. On other surfaces of the same sample as figure 11 there were characteristic rounded surface features reminiscent of those (figure 2) identified as sites of bubble escape through a viscous fluid medium. (Scale bar: 10 µm.)

of lattice order. This material progressively hardens on cooling, retaining structural water in a vitreous phase. Thus dehydration may result in the development, locally within the residue, of diverse minor structural variations identified when cold as a glassy phase. Some inhomogeneity in physical properties can be expected, notably at surfaces from which water is preferentially lost, through the generation of a superficial skin.

At dehydration temperature the reactant can be regarded as a molten phase from which water is lost through surfaces. Internal bubbles are expected to migrate to expel the gaseous product ($H_2O$) and intermittently penetrate the skin by a process similar to boiling.

### (*b*) *Reaction stoichiometry*

The reactant weight loss and pressure of gas evolved in the calibrated volume of the apparatus on completion of reaction, 430–460 K (15 quantitative measurements for both crystal and powder reactants) were entirely in accordance with expectation for:

$$LiKC_4H_4O_6 . H_2O \rightarrow LiKC_4H_4O_6 + H_2O.$$

Pressure measurements were the more accurate (±3%). More than 97% of the volatile substance was condensed with a 213 K cold trap, confirming that there was no appreciable anion decomposition to yield product CO or $CO_2$.

### (*c*) *Thermal analysis*

Preliminary measurements to determine the reaction temperature were undertaken using a Perkin-Elmer TGA7 thermogravimetric analyzer and a Perkin Elmer DSC7 Differential Scanning Calorimeter. Samples were heated at 5 K $min^{-1}$ in nitrogen.

A typical differential thermogram is shown in the upper (interrupted) line in figure 13 for *dl* lithium potassium tartrate monohydrate. Included in the same diagram (the full line) is the differential scanning calorimeter (DSC) response for (a different sample of) the same reactant. From both curves it is seen that there is the slow endothermic

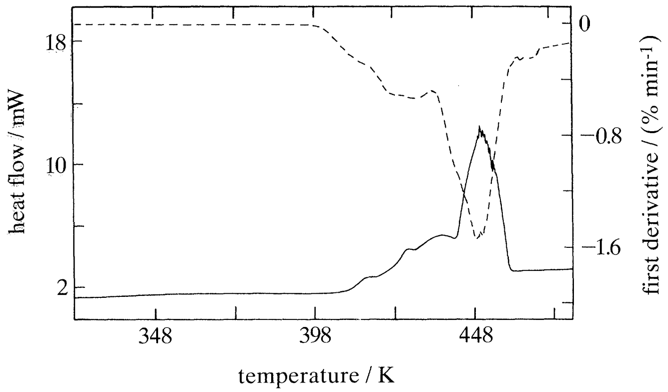

Figure 13. Typical differential thermogravimetric (DTG) trace (interrupted line) and differential scanning calorimetric (DSC) trace (full line) for the non-isothermal dehydration of crushed crystals of *dl* lithium potassium tartrate monohydrate. DTG: sample weight 9.66 mg, 5 K $\text{min}^{-1}$, $N_2$ flow 80 $\text{cm}^3\ \text{min}^{-1}$. DSC: sample weight 11.69 mg, 5 K $\text{min}^{-1}$, $N_2$ flow 40 $\text{cm}^3\ \text{min}^{-1}$.

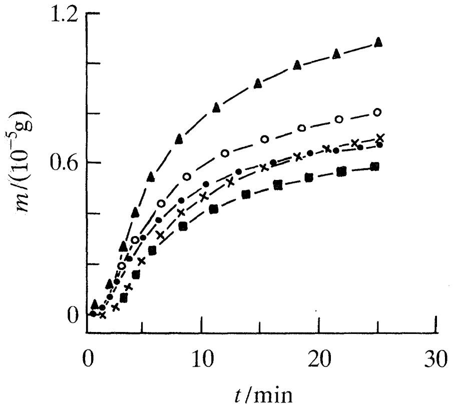

Figure 14. Plots of weight loss against time for the earliest stages of the isothermal dehydration of *dl* lithium potassium tartrate monohydrate. Measured using the quartz crystal microbalance in vacuum ($7 \times 10^{-5}$ Pa) at the following isothermal reaction temperatures: 351.6 K(○), 361.5 K(■), 371.6 K(●), 381.0 K(×) and 393.0 K(▲).

onset of water evolution 400–437 K, followed by a more rapid reaction between 437–455 K; the irregularities in the response are attributable to melting and bubble formation. In further DSC measurements the salt was rapidly heated to 440 K, rapidly cooled to 290 K and on reheating there was no evidence of the slower initial process. This single endotherm is identified as dehydration in a melt without the precursor stage.

The thermogravimetrically measured weight loss between 400–465 K, 8.1%, agrees well with expectation for dehydration of the monohydrate, 8.5%. Above 465 K the second endotherm, peak maximum at 507 K, is identified as anion decomposition (and will be the subject of a future study). The hydration enthalpy, measured from DSC data, was $-34 \pm 2$ kJ $\text{mol}^{-1}$.

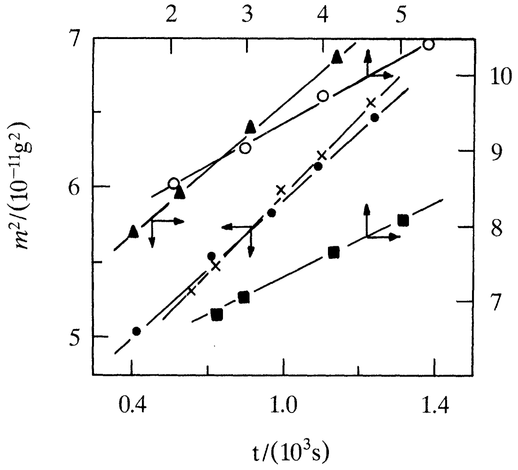

Figure 15. Plots of (weight loss)$^2$ against time for the data in figure 14: linearity is evidence of diffusion control.

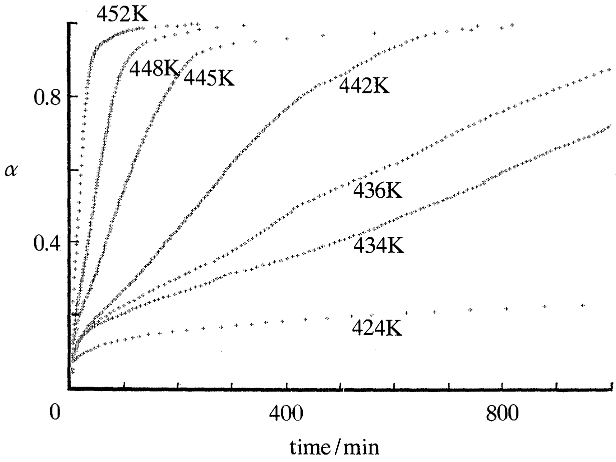

Figure 16. Typical fractional reaction ($\alpha$)-time curves for the isothermal dehydration of single crystals of *dl* lithium potassium tartrate monohydrate.

Table 1. *Diffusion coefficients measured for the earliest stage in water loss during isothermal dehydration of dl lithium potassium tartrate monohydrate single crystals*

| | diffusion coefficient $D_{\text{eff}}$ |
|---|---|
| temperature/K | $10^{-11}$ cm$^2$ s$^{-1}$ |
| 351.6 | 0.58±0.01 |
| 361.5 | 0.70±0.01 |
| 371.6 | 1.28±0.02 |
| 381.0 | 1.37±0.02 |
| 393.0 | 2.85±0.04 |

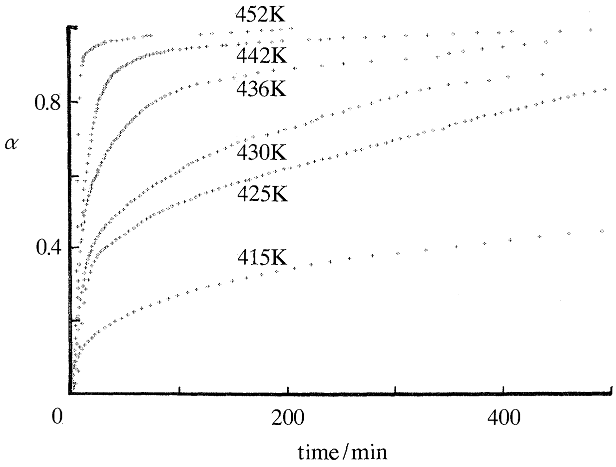

Figure 17. Typical $\alpha$-time curves for the isothermal dehydration of crushed powder *dl* lithium potassium tartrate monohydrate.

### (*d*) *Dehydration kinetics*

#### (i) *Weight loss measurements*

Typical weight loss against time plots for the very earliest stages of the isothermal dehydration of *dl* lithium potassium tartrate monohydrate crystals, using the quartz crystal microbalance, are shown in figure 14. The deceleratory behaviour observed appears to be characteristic of diffusion control, a conclusion that is supported by the linear plots of (weight loss)$^2$ against time, given in figure 15. Diffusion coefficients calculated from these data are reported in table 1. This appearance of an initial deceleratory process is similar to behaviour found for the *d* salt (Galwey & Okhotnikov 1988) for which the diffusion coefficients are closely comparable. These similarities will be considered further in Laverty *et al.* (1992).

We conclude (Galwey & Okhotnikov 1988) that the onset of dehydration of the *dl* salt proceeds with the development of a vacancy structure at water-accommodating sites within the reactant permitting outward diffusive migration of water molecules through the superficial crystal layer. The total contribution of this reaction to the overall dehydration of the *dl* salt is small, resulting in the release of an estimated 0.4 % ($\alpha = 0.004$) of the constituent water from an average reactant crystal as a consequence of the dehydration of a thin boundary layer of thickness 1.5 μm. (The comparable reaction for the *d* salt corresponded with the dehydration of a boundary layer of *ca.* 10 μm thickness.) The extent of this reaction was, therefore, too small to permit study of thermogravimetric or gas evolution measurement, and the upper temperature interval of investigation was limited by the onset of melting at *ca.* 400 K.

#### (ii) *Water evolution measurements*

Representative fractional reaction $\alpha$-time graphs for the isothermal dehydration of *dl* lithium potassium tartrate monohydrate crystals are given in figure 16 (424–452 K) and for crushed powder in figure 17 (415–452 K). These kinetic studies were obtained through measurement of $\alpha$ from the pressure of water evolved in the constant volume apparatus. Close similarities were evident between the behaviour of both forms of the reactant, though the dehydration of the powder was perceptibly more rapid.

Table 2. *Dehydration of dl lithium potassium tartrate monohydrate*
(Mean $\alpha$ ranges of reaction exhibiting different types of kinetic behaviour.)

| | crystal | | powder | |
|---|---|---|---|---|
| process | $\alpha$ range | temperature/K | $\alpha$ range | temperature/K |
| diffusion | 0–0.004 | 350–393 | — | — |
| initial | 0–0.06 | 380–440 | 0–0.06 | 415 |
| | 0–0.10 | 440–450 | 0–0.12 | 430 |
| deceleratory | 0.08–0.20 | 420–435 | 0.08–0.40 | 415 |
| | 0.12–0.20 | 440–450 | 0.14–0.55 | 430 |
| zero order | 0.18–0.80 | 425–460 | 0.5–0.85 | 415–450 |
| first order | 0.6–0.9 | 440–460 | 0.70–0.93 | 415–450 |

Rate processes were predominantly deceleratory: the following kinetic states in the overall dehydration were distinguished. The *initial process* was followed by a *deceleratory process* during which the rate progressively diminished to a value that remained approximately constant during the subsequent *zero-order process*, and this finally led into the *first-order process* which occurred as dehydration approached completion. Mean values of the $\alpha$ ranges during which these rate processes applied are summarized in table 2 for both crystals and crushed powder reactants.

At the highest temperatures studied (greater than 450 K) there was a small amount of overlap of the first-order stage of the dehydration reaction with the onset of anion decomposition, which yielded water and carbon dioxide. Care was taken to exclude from consideration all kinetic data in which there was a significant contribution from anion breakdown.

*The initial process.* During reactant heating and immediately following attainment of reaction temperatures (420–440 K) the salt rapidly evolved $6 \pm 1\%$ of the constituent water. Studies in a lower temperature range (380–390 K) showed that this process proceeded at a constant rate that abruptly became too slow for kinetic studies at $\alpha = 0.06$, where dehydration effectively ceased. The extent of the diffusion dehydration process (studied below 393 K, table 1) was small ($\alpha < 0.004$) and this could not be distinguished in the pressure studies. Above 445 K, temperature variations during reactant heating made quantitative measurements unreliable; this process was completed at $\alpha = 0.05$ in 5 min.

The behaviour of powders was very similar. The yield from this first process was (again) completed at $\alpha = 0.06$ between 370 and 415 K, rising appreciably to $\alpha = 0.12$ at 430 K and kinetic studies became unreliable above 440 K.

As shown by the electron microscopic and DSC studies, this water release was accompanied by reactant melting. Significantly, and unlike the behaviour of the *d* salt which did not melt, the amount of water evolved in this initial rapid process was not related to the reactant surface area. Yields from crystals and powder samples were similar. This process is, therefore, identified as the evolution of loosely bonded water, released on relaxation of lattice order by fusion. It is suggested that disorder resulting from melting yields a structure in which the quantity of water accommodated is somewhat less than the requirements of the crystalline monohydrate. The ease of this initial water evolution, overlapping with melt formation, made kinetic investigations impracticable.

*The deceleratory process.* Following the initial rapid evolution of water, the dehydration rate progressively decelerated to a value that remained constant,

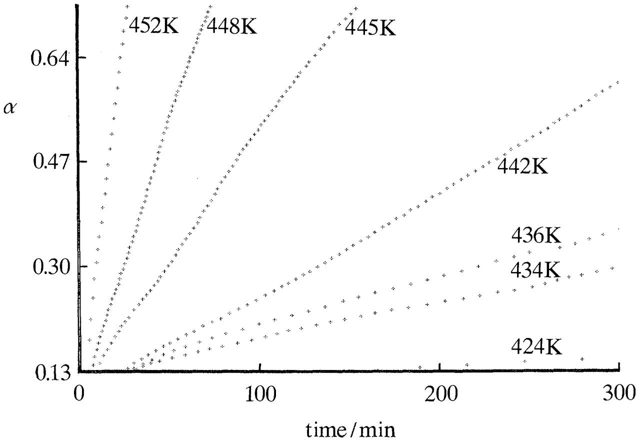

Figure 18. The zero-order reaction interval for the data on figure 16, for the isothermal dehydrations of single crystal reactants.

continuing thereafter as the zero-order process. In crystals the deceleratory process was completed at $\alpha = 0.20$, figure 16. The rate was sensitive to temperature; dehydration $0.01 < \alpha < 0.02$ required *ca.* 500 min at 420 K but only 20 min at 440 K. Compared with crystals, the deceleratory process during powder dehydration constituted a greater proportion of the reaction (see table 2 and figures 16 and 17) extending to $\alpha = 0.4$ at 415 K and to 0.55 at 430 K (figure 17). This relatively greater yield is ascribed to differences in surface area of the fused reactants. The microscopic observations show that partly reacted fused powder contains larger numbers of internal pores than similarly treated crystals (compare figure 6 with figures 7, 9 and 10). Thus the contribution from the internal surfaces satisfactorily accounts for the differences in extents of this stage of reaction.

The deceleratory phase of reaction is ascribed to preferential water removal from a superficial layer of the reactant particle within which the ease of water escape progressively diminishes as the concentration of water in this superficial layer decreases. Additionally, there may be changes in the vacancy structure of the water accommodating sites within that zone, and these are expected to influence the rate of $H_2O$ molecule diffusion towards the surface, before desorption. Dehydration in the outer layer represents progress towards the structure of the anhydrous product, presumably involving compaction as a result of increased interanionic hydrogen bonding which reduces the ease of water movement. The generation of a superficial dehydrated layer has also been recognized to be an important feature in the dehydration of *d* lithium potassium tartrate monohydrate (Laverty *et al.* 1992).

*The zero-order process.* The dominant feature of single crystal isothermal dehydration α-time plots (figure 16) was the extended period of constant rate of water evolution between $0.18 < \alpha < 0.8$ (average range measured in 200 experiments). The extent of this process showed no systematic variation with temperature throughout the interval of these kinetic studies, 425–460 K. Obedience of the data in figure 16 to the zero order equation is illustrated in figure 18. Some irregularities from constancy in the rate of gas evolution were evident, plots of $d\alpha/dt$ against $\alpha$ also showed rate variations which are attributed to a discontinuous release of water vapour by the bursting of bubbles of various sizes. The magnitude of the activation energy calculated from the mean zero-order rate constants was relatively larger,

$330 \pm 20$ kJ mol$^{-1}$, than was anticipated for a hydration reaction in a fluid medium.

The zero-order rate process was also evident in the reaction of crushed crystals, though it was maintained across a much reduced interval, $0.55 < \alpha < 0.85$, as a consequence of the more extensive deceleratory process that preceded it. The activation energy was again high, $312 \pm 30$ kJ mol$^{-1}$. This agrees, within experimental error, with the value for the crystals and confirms the occurrence of the same process in the two forms of the reactant. The rate of dehydration of the powder was, however, significantly greater than that of the crystals at the same temperature (eight and a half times).

*The first-order process.* The final stages of the dehydrations of both single crystal and crushed powder reactants were deceleratory and both obeyed the first order equation between *ca.* $0.65 < \alpha <$ *ca.* 0.92 (table 2). Typical first order plots for crystal dehydrations, $0.53 < \alpha < 0.87$, are shown in figure 19. Care was taken to minimize any contribution to product formation from the onset of the subsequent anion breakdown reaction and this may have curtailed the upper limit of first-order obedience reported.

Calculated activation energy values for dehydrations of crystals and of powder were again high, $340 \pm 30$ kJ mol$^{-1}$, close to the values for the zero-order process and again the rate of the reaction of the powder was the more rapid (eight times). We conclude from this kinetic evidence, therefore, that the factors controlling this first-order process are the same as those applicable to the zero-order rate process subject to the additional constraint of a diminution of rate as dehydration approaches completion.

Dehydration always proceeded to completion, yielding the anhydrous product. There was no evidence, throughout the temperature interval investigated, that equilibrium was established between water vapour and $H_2O$ molecules retained by the residue. The anhydrous glassy phase (Baranov *et al.* 1990) was the residual product.

### (iii) *The dehydration mechanism*

As pointed out in the introduction it may be possible, from a consideration of the kinetic characteristics of this reaction, to determine whether dehydration occurs homogeneously throughout the melt or alternatively is controlled by water release from surfaces only. The applicability of both models to the present observations are critically examined below.

*Homogeneous reactions.* Salt dehydration can be regarded as a homogeneous reaction only if both the following conditions are fulfilled. First, the release of water must occur with equal probability at every site throughout the reactant particle. This is a rate limiting step whereby the $H_2O$ molecules, strongly bonded within the reactant structure, undergo bond redistributions which transform them into less strongly held water that is the mobile interstitial species. Secondly, such mobile water must migrate relatively rapidly to particle surfaces from which it is readily desorbed. The rate of water evolution proceeding by this general mechanism is expected to depend on reactant *concentration*, obeying the first-order equation or other expression based on concentrations of participating reactant entities. The present kinetic evidence, notably the extended zero-order process, is not consistent with this reaction model. Moreover, it seems intrinsically improbable that water released within a homogeneous reactant would escape rapidly, readmission to the

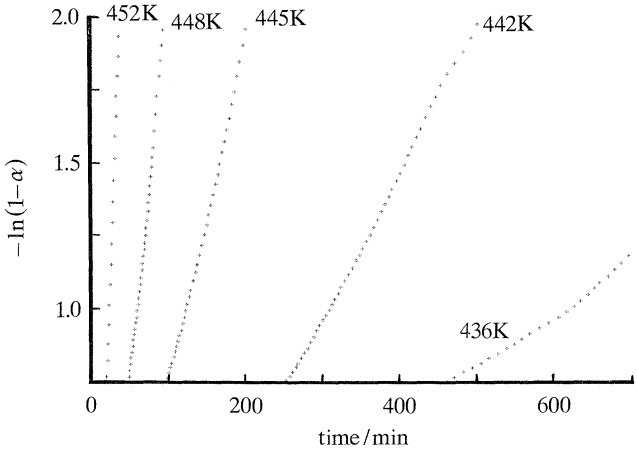

Figure 19. First-order plots for the final dehydration process of single crystals for some of the experiments shown in figure 16.

bonded state would appear to be highly probable. We conclude, therefore, that the kinetic pattern of this reaction, in the solvent-free melt, does not behave as a homogeneous reaction.

*Interface reactions*. Equations of the types that have been widely and successfully used in kinetic analyses of the dehydrations (and other reactions) of solids (Brown *et al*. 1980) can be applied to the present reaction of a melt only if zones of different structures and/or reactivities participate. Considering the present reaction from this perspective requires the reactant to be regarded as heterogeneous: variations in composition and/or bonding are an essential prerequisite for the development of a chemically active interface.

Studies of the *d* salt (Laverty *et al*. 1992) showed that the initial dehydration resulted in diffusion controlled water loss from a crystal surface layer corresponding to a thickness of *ca*. 10 μm. During the subsequent reaction, water evolved from the centre of the solid crystals bubbled through this apparently molten surface layer. This is identified as a two-phase system.

For the present *dl* salt heterogeneity of the reactant can be envisaged as an agglomeration composed of two (or more) structurally distinct materials in which long range (crystallographic) order has been lost. Both components may incorporate structural diversity by alternative local hydrogen bonding dispositions together with some mobility of constituent ions within a glass-like structure. To discuss reactant kinetic behaviour we postulate two phases: hydrated and dehydrated salt.

*Hydrate*. This is a reactant in which dehydration has not proceeded appreciably, water losses have resulted in the appearance of some vacancies at water-accommodating sites. The remaining constituent water is strongly held, probably at sites and structures comparable with those in the original crystalline material but some local bond reorganization has resulted in loss of long-range order.

*Dehydrated salt*. Extensive water loss will be accompanied by the appearance of the structure characteristic of the anhydrous product which hardens on cooling to a glass-like phase that is amorphous to X-rays (Baranov *et al*. 1990). This material, containing hydroxyl and carboxyl groups, is expected to be hydrophilic and may, therefore, accommodate a limited amount of water. Such $H_2O$ molecules, retained within dehydrated structure, are presumably held interstitially by relatively weak bonding forces. This water, by analogy with the superficial dehydrated fused or glassy phase of the *d* salt, is mobile and readily volatilized following diffusive migration to surfaces.

We propose the following two mechanistic explanations of the observed pattern of kinetic behaviour: the early deceleratory process is followed by a period of constant reaction (extensive in the single crystal reactant) with a further diminution in rate (first-order behaviour) as dehydration is completed. The alternative reaction models described below are based on theory applied to heterogenous processes. Behaviour intermediate between these alternatives can also be envisaged.

*Two phase equilibrium* (*Scheme I*)

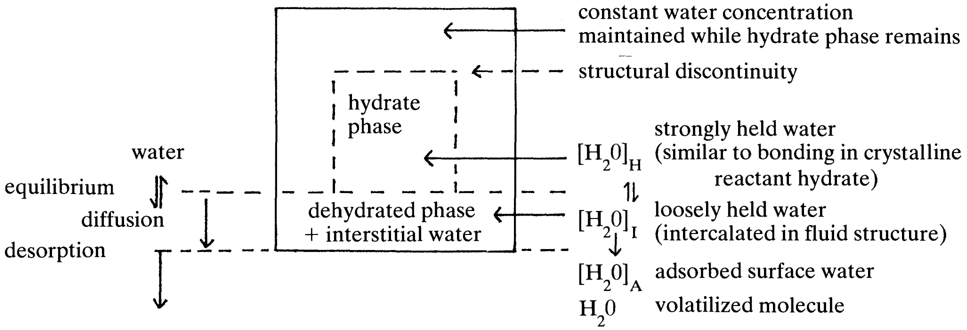

Diagrammatic representation of 'two phase equilibrium' reaction mechanism.

The presence of a 'hydrate' phase, relatively water rich and maintaining structural similarities with the original reactant, maintains a small but constant water concentration in the dehydrated phase (bearing a formal similarity to a vapour pressure). The overall rate of melt dehydration is determined by loss from the constant concentration water molecule reservoir.

The diagram is not intended to imply any geometric control of rate, the hydrated phase may be divided and dispersed throughout the reactant particle.

On this proposed mechanism, the reactant, having completed the deceleratory process, is represented as zones of hydrate phase embedded within a coherent dehydrated salt matrix which contains a small proportion of interstitial water. The distribution of water between these components can be regarded as analogous to a solid-gas equilibrium. The low concentration of interstitial water in the dehydrated salt is expected to be maintained constant while the hydrate phase remains: this is analogous to the presence of vapour over a liquid. Water evolution, following migration of $H_2O$ molecules to particle surfaces, must occur at a rate that is slower than its replacement from the hydrate phase. Volatilization from the constant $H_2O$ concentration in the dehydrated material explains the zero-order reaction rate.

During the early stages of the deceleratory reaction, water is lost from the reactant hydrate but this rate diminishes towards the zero order value as the dehydrated phase is generated. This will appear at outer surfaces first, following water loss and the rate is then controlled by evolution from the material containing the lower but constant water concentration, the dehydrated salt.

The relatively larger extent of the deceleratory reaction for powders is ascribed to the greater participating active surface area. The same explanation accounts for the greater rate of the zero-order reaction for powders where there is a contribution from bubble formation through which water is lost from internal surfaces.

PHILOSOPHICAL TRANSACTIONS OF THE ROYAL SOCIETY A MATHEMATICAL, PHYSICAL & ENGINEERING SCIENCES

*Surface boundary layer* (*Scheme II*)

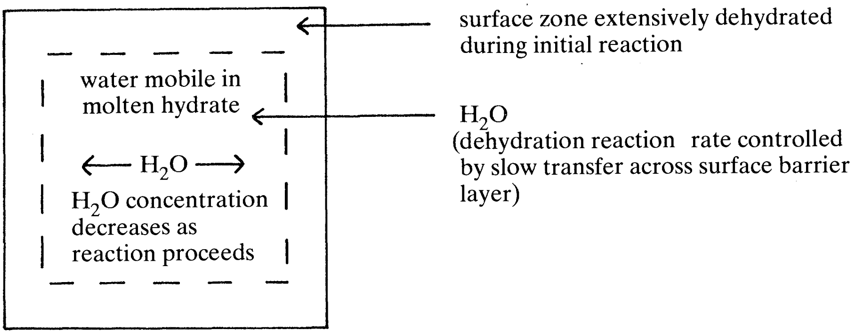

This is a diagrammatic representation of 'surface boundary layer' reaction mechanism. On this model water is regarded as mobile within the bulk of the molten reactant particle. The rate of dehydration is determined by the relative difficulty of diffusive migration, followed by desorption, across the surface barrier layer. Surface water losses occur from the outer zones of reactant during the early deceleratory stage of dehydration.

The essential feature of this mechanism is that water evolution is controlled by diffusive migration, from a relatively high water concentration within the reactant particle centre, across a dehydrated layer that has lost constituent water early in the reaction and later constitutes a constant barrier layer to product escape. Water and water vacancy mobility in the particle interior is high (Baranov *et al.* 1990) but migration in the immediate vicinity of the surface is relatively slow. Quasi steady state conditions are established during the constant rate of water evolution. This model is formally similar to that proposed by Franklin & Flanagan (1972) for the linear rate of dehydration of single uranyl nitrate hexahydrate crystals except that we identify, in our reactant, a surface barrier layer whereas the slow step in the hexahydrate is desorption of water from the surface. Both models consider the mobility of water within the reactant bulk to be sufficiently rapid to maintain a constant concentration below the barrier layer or surface.

The early deceleratory phase of reaction occurs during the establishment of the barrier layer that progressively slows the initial reaction rate to a value that is maintained constant thereafter.

The relatively more rapid reaction rate in the melt derived from fused powder is ascribed to the larger area of active surface from which water desorption occurs. This includes the generation of intraparticulate bubbles through which water released into internal pores escapes by plastic flow opening channels that enable accumulated steam to escape.

*The first-order reaction.* On both heterogeneous models described above, this final stage of reaction is ascribed to concurrent influences of diminishing concentration of water in the reactant and a reduced ease of diffusion to outer surfaces. The role of these controls are somewhat different for the alternative mechanisms described above but together may be expected to exhibit approximately first order kinetics.

### (iv) *The activation energy*

Kinetic data for most thermal reactions of solids satisfactorily obey the Arrhenius equation. There are, however, uncertainties in the theoretical interpretation of measured activation energies ($E$) because the energy distribution function within a solid is different from that in the homogenous phase (Brown *et al.* 1980). Values of $E$ are not always readily identified with a specific rate limiting step.

For the present reaction, the large apparent activation energy, *ca.* 330 kJ mol$^{-1}$, cannot be identified with the strength of water retention in the hydrate phase. The magnitude of $E$ can, however, be regarded as a composite value and this is evidence that dehydration proceeds through a sequence of interlinked temperature-dependent steps that together culminate in water evolution. The high value of $E$ is consistent with both of the heterogeneous mechanisms proposed above.

*Two-phase equilibrium.* The equilibrium concentration of water retained in the dehydrated phase is expected to be temperature dependent (cf. water vapour pressure) as also are the water mobility and desorption. The contributions are expected to be exponentially dependent on reciprocal temperature. Thus the overall calculated value of $E$ is the sum of components which cannot be estimated individually from the present data.

*Surface boundary layer.* The rate of transfer of water across the barrier peripheral layer will be dependent on its effective viscosity, the thickness of the layer and possibly the quantity of water retained within this zone. The overall magnitude of $E$ will include the sum of these individual contributions together with the desorption energy.

We conclude that the $E$ value is composite, incorporating contributions from ease of water release, migration in and desorption from the hydrogen bonded glass-like structure.

## 4. Conclusions

We conclude that the dehydration of *dl* lithium potassium tartrate monohydrate in the fused state does not exhibit the kinetic characteristics of a homogeneous reaction. The rate behaviour is consistent with the participation of two phases of molten or glassy materials. Water removal is believed to introduce inhomogeneity into the reactant and loss of long-range order is ascribed to the interconversion of two or more alternative hydrogen bonded structures of comparable stability resulting from some bond mobility in a vitreous phase. The observation that there are three kinetic stages in dehydration (deceleratory, constant rate, deceleratory) is evidence that sufficient inhomogeneity is generated within the condensed phase to exert a control on rate characteristics. This conclusion is consistent with the X-ray and microscopic observations together with the evidence (Laverty *et al.* 1992) that there is superficial but not bulk melting of the *d* salt in a similar temperature range.

Heterogeneity in the present reactant is identified as yielding effectively either a constant interstitial water concentration and/or a constant surface barrier to water release. The reaction of this molten or vitreous salt is, therefore, identified as a reaction type that develops heterogeneity and exhibits features that differ from those well established patterns of behaviour that have been described for many other dehydrations (Brown *et al.* 1980). No advancing interface could be found and the controls described and discussed here are difficult to characterize individually and quantitatively. The subject is, however, important because the participation of melting in reactions of solids is not always easily recognized. The occurrence of fusion is clearly a most important aspect of behaviour which must be considered in the formulation of reaction mechanisms and in the theoretical discussion of the reactivities of crystalline materials. Several recent studies have provided evidence that there is local or temporary participation of a melt or liquid phase in a reaction that has previously been regarded as proceeding in the solid state: alum dehydrations (Galwey *et al.* 1981), the thermal decompositions of copper II malonate (Carr & Galwey 1986), of $NH_4ClO_4$ (Galwey & Mohamed 1984) and of $(NH_4)_2Cr_2O_7$ (Galwey *et al.* 1983) and the reaction $KBr + Cl_2$ (Galwey & Poppl 1984). This paper is intended to draw attention to the behaviour of *dl* lithium potassium tartrate monohydrate which exhibits the characteristics of a heterogeneous rate process.

We thank Dr W. Surer (Perkin-Elmer, AG, Kuesnacht, Switzerland) for DSC and TG measurements and Dr B. I. Kidyarov (Institute of Solid State Chemistry, Novosibirsk) for help in the preparation of single crystals of the present reactant. S.D.B. thanks the Association of Commonwealth Universities for the award of a Fellowship during which this work was carried out. G. M. L. thanks the Department of Education for Northern Ireland for the award of a Postgraduate Scholarship and the Academy of Sciences of the U.S.S.R. for an invitation visit to Novosibirsk, V. B. O. thanks the Queen's University of Belfast for an invitation to visit Belfast. A. K. G. thanks SERC for a grant for the purchase of the optical microscope used in this study. We thank Mr J. McCrae and the Staff of the Electron Microscopy Unit for help and advice in obtaining the electron micrographs.

## References

Baranov, N. A., Okhotnikov, V. B., Rynskaya, L. I., Semenov, A. R., Laverty, G. M. & Galwey, A. K. 1990 *Solid St. Ionics* **43**, 37.

Brown, M.E., Dollimore, D. & Galwey, A. K. 1980 *Comprehensive chemical kinetics*, vol. 22. Amsterdam: Elsevier.

Carr, N. J. & Galwey, A. K. 1986 *Proc. R. Soc. Lond.* A **404**, 101.

Franklin, M. L. & Flanagan, T. B. 1972 *J. chem. Soc. Dalton Trans.*, p. 192.

Galwey, A. K. & Laverty, G. M. 1990 *J. Chim. phys.* **87**, 1207.

Galwey, A. K. & Mohamed, M. A. 1984 *Proc. R. Soc. Lond.* A **396**, 425.

Galwey, A. K. & Okhotnikov, V. B. 1988 *J. thermal Analysis* **33**, 441.

Galwey, A. K. & Poppl, L. 1984 *Phil. Trans. R. Soc. Lond.* A **311**, 159.

Galwey, A. K., Poppl, L. & Rajam, S. 1983 *J. chem. soc. Faraday Trans.* I **79**, 2143.

Galwey, A. K., Spinicci, R. & Guarini, G. G. T. 1981 *Proc. R. Soc. Lond.* A **378**, 477.

Garner, W. E. 1955 *Chemistry of the solid state* (ed. W. E. Garner), ch. 8. London: Butterworth.

Guarini, G. G. T. & Rustici, M. 1987 *React. Solids* **2**, 381.

Laverty, G. M., Galwey, A. K., Baranov, N. A. & Okhotnikov, V. B. 1992 (In the press.)

Okhotnikov, V. B. & Lyakhov, N. Z. 1984 *J. Solid St. Chem.* **53**, 161.

Okhotnikov, V. B., Petrov, S. E., Yakobson, B. I. & Lyakhov, N. Z. 1987 *React. Solids* **2**, 359.

*Received 8 May 1991; accepted 3 June 1992*

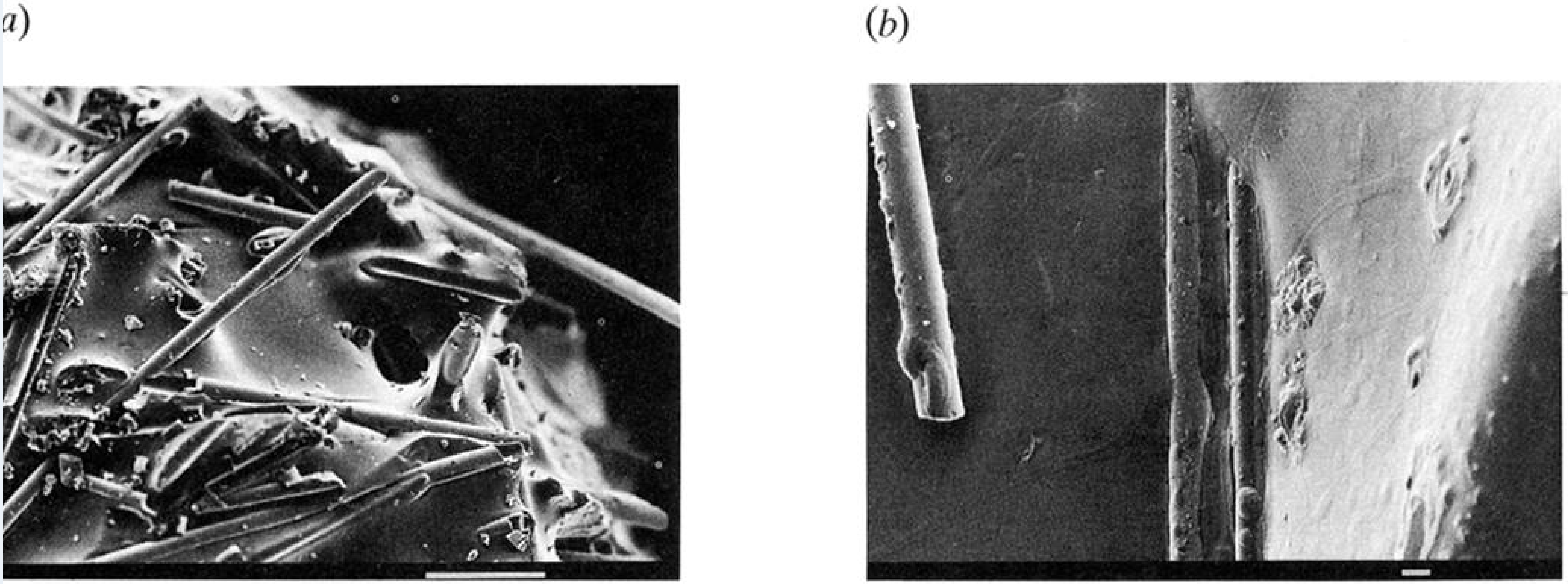

gure 1. External surface of a partly dehydrated crystal of *dl* lithium potassium tartrate onohydrate ($\alpha = 0.33$ at 450 K). Reactant melting is demonstrated by the wetting of glass wool res which are retained, embedded in the residue, which hardened on cooling. (Scale bars: (*a*) 0 µm; (*b*) 10 µm.)

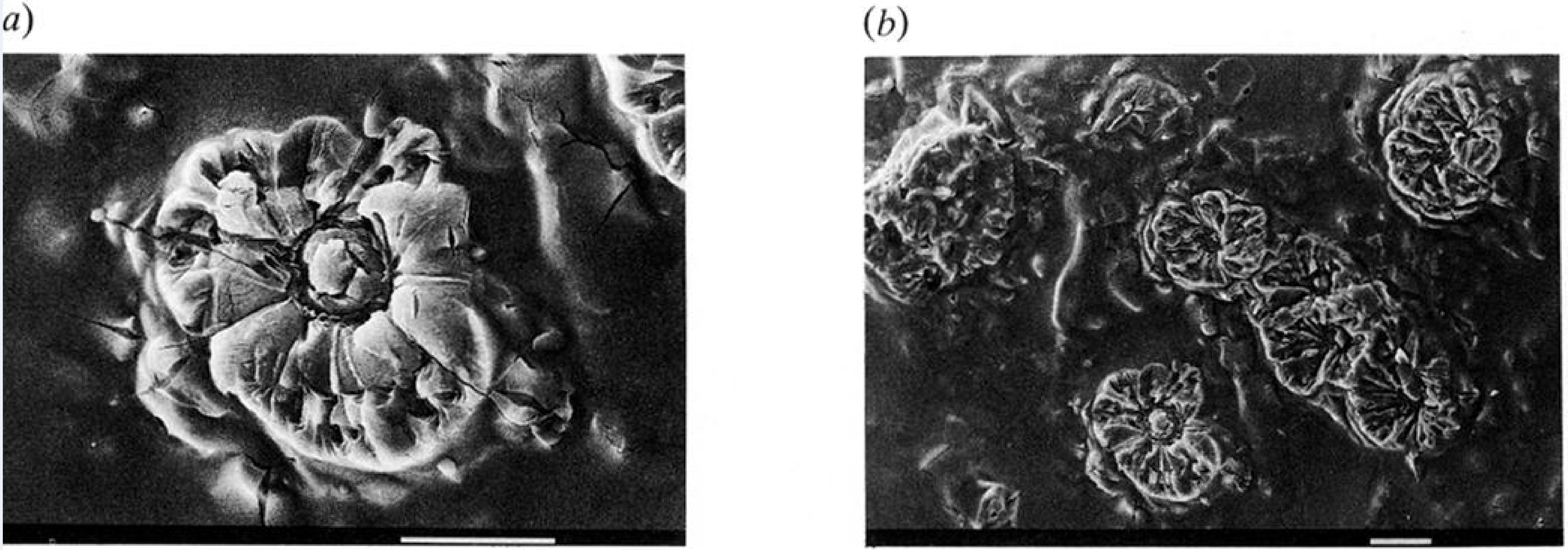

gure 2. Characteristic surface textural features found on surfaces of partially dehydrated crystals = 0.43 at 453 K). These features are identified as sites of collapsed bubbles acting as vent holes r the escape of steam from intracrystalline pores within which the volatilized water is temporarily tained. (Scale bars: both 10 μm.)

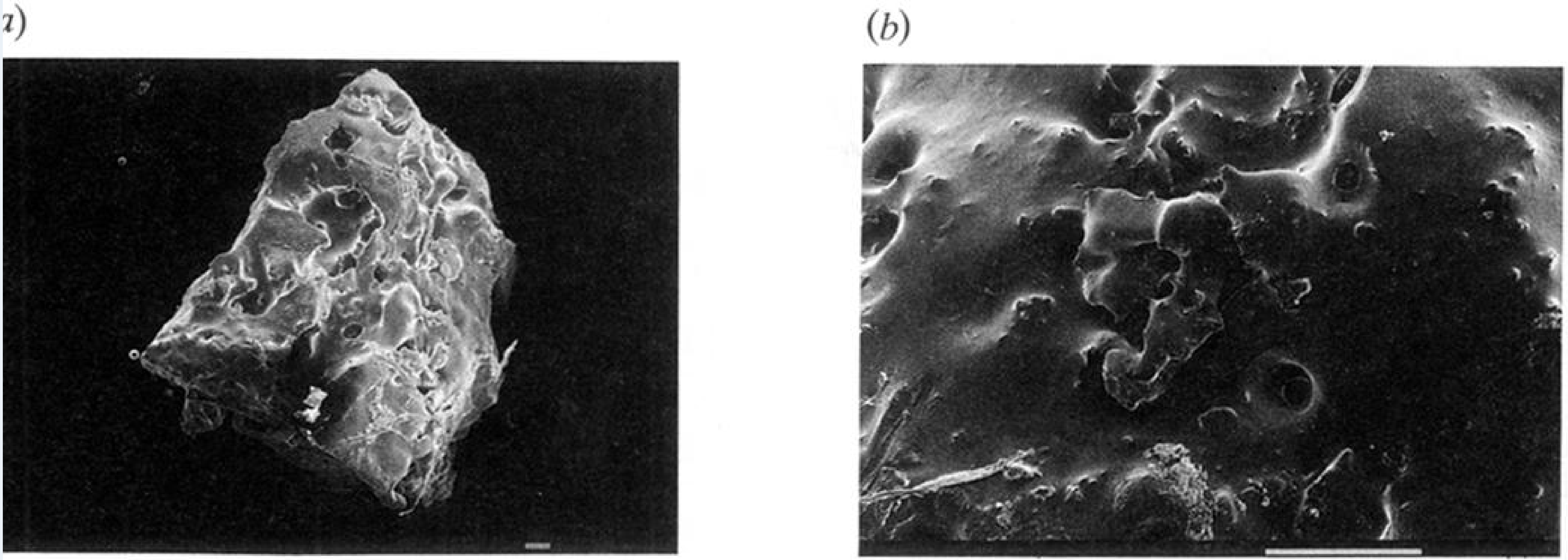

gure 3. Surface texture of dehydrated salt ($\alpha = 1.00$ at 453 K); the flat surface characteristic of e original reactant crystals has been lost. The outer boundary faces of the crystal have become vered with rounded features, indicative of surface tension control operating in the molten actant surface during water loss. (Scale bars both: 100 μm.)

Figure 4

Figure 5

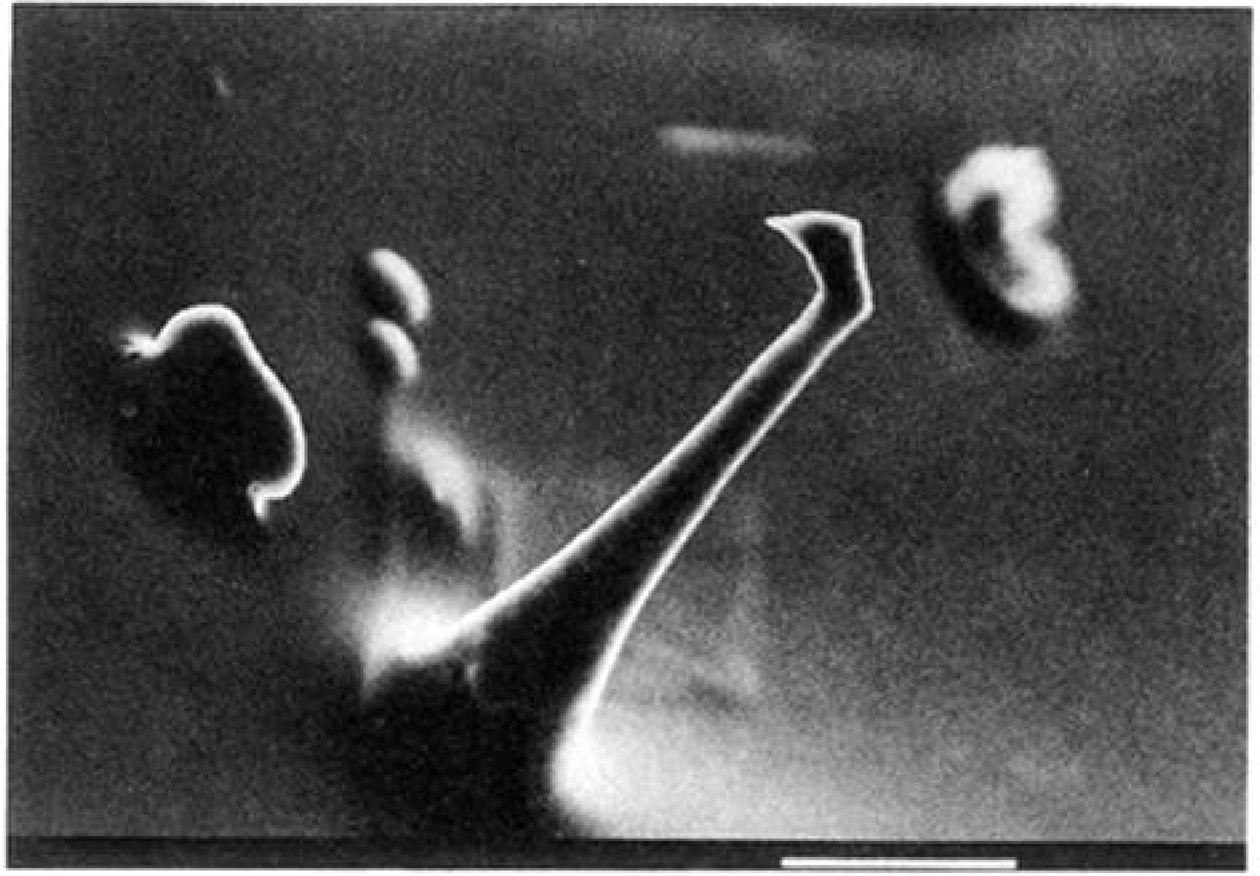

gure 4. After limited dehydration ($\alpha = 0.1$ at 442 K) the surface of this crystal gives evidence of crystallization on cooling. (Scale bar: 10 μm.)

gure 5. This feature, unique in the present work, is interpreted as evidence of superficial melting which the viscous boundary phase has been pulled outwards during temporary attachment to erhaps) a glass fibre. (Scale bar: 10 μm.) ($\alpha = 0.33$ at 450 K.)

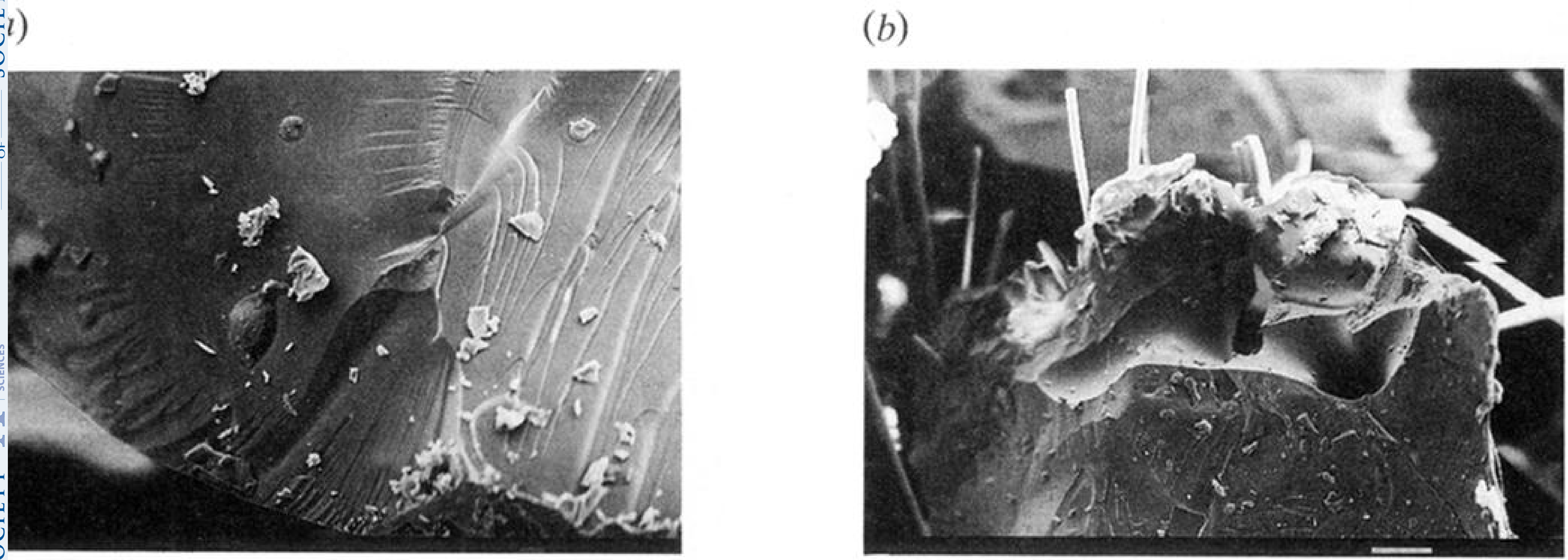

gure 6. Sections of reactant crystal cleaved after partial dehydration, $\alpha = 0.50$ at 438 K. Some eas in (*a*) resembled the exposed faces of cleaved reactant crystals; there was no evidence of cleus development and no features other than cleavage step edges were found. Other areas in (*b*) cluded large pores and retained embedded glass fibres. (Scale bars: (*a*) 10 µm; (*b*) 100 µm.)

igure 7

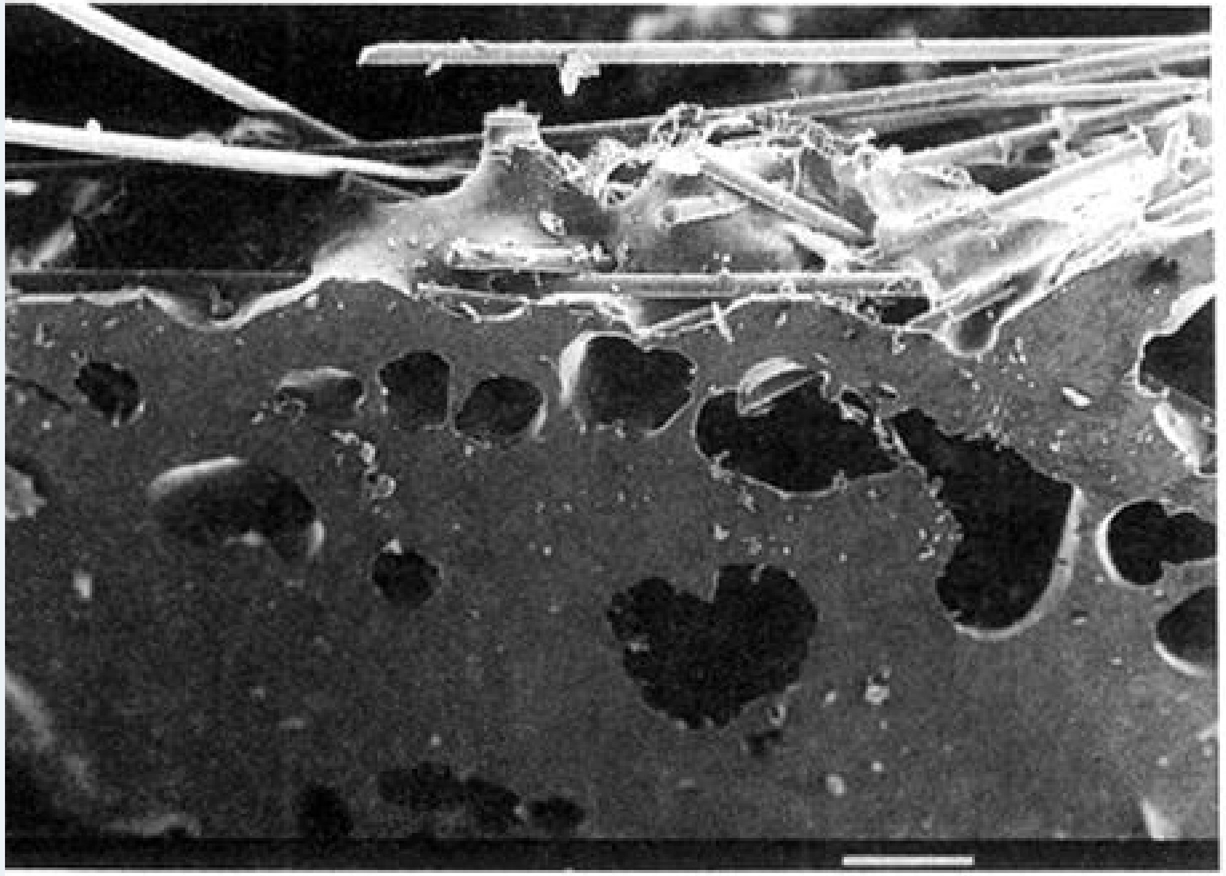

Figure 8

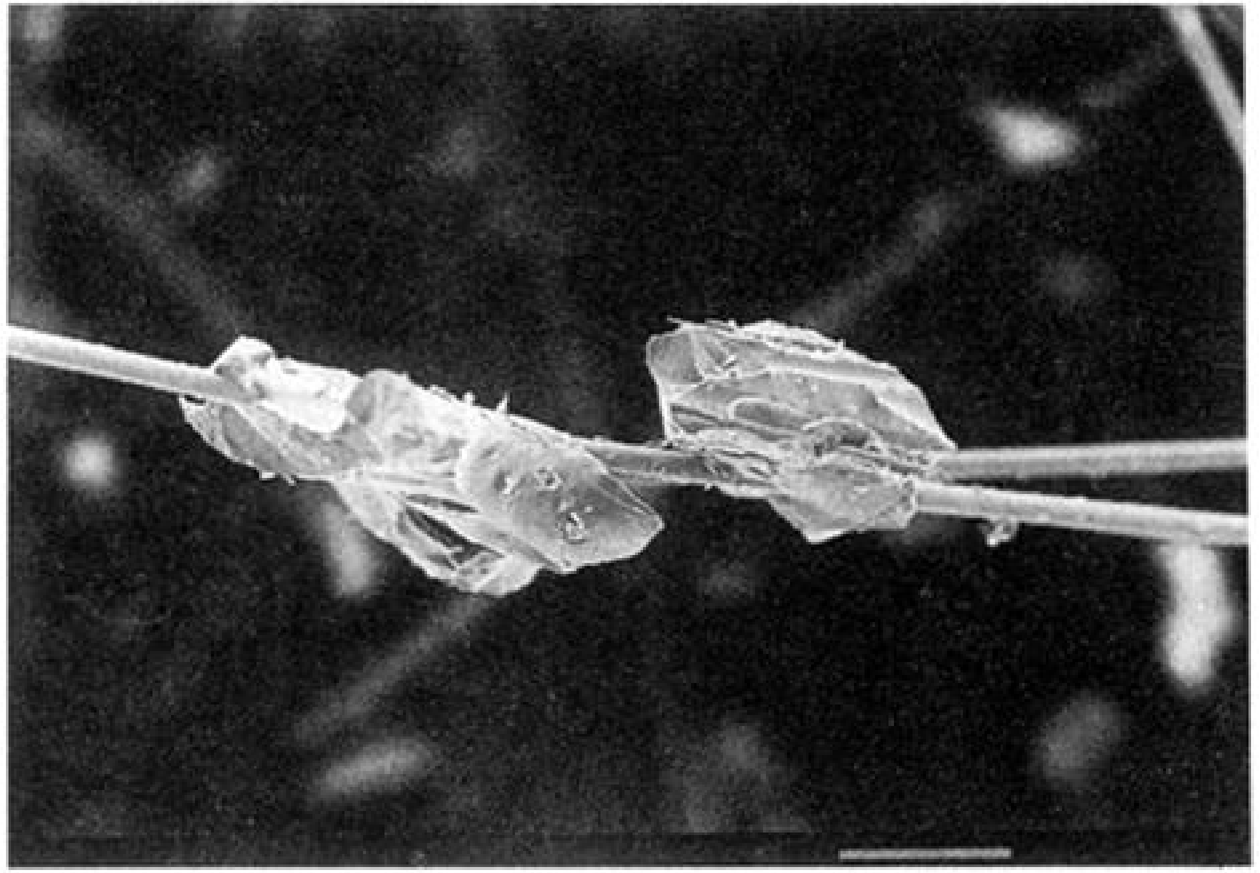

igure 7. Aggregate large particle formed by sintering of powder sample after partial dehydration $\alpha = 0.60$ at 437 K. The flat surface in the lower part of the photograph is material that adhered the glass wall of the containing vessel and in the upper part the retention of embedded glass res is seen. (Scale bar: 100 μm.)

igure 8. Same sample as figure 7, some small particles remain attached, following fusion, to glass ool fibres (used to retain sample in the reaction tube). (Scale bar: 100 μm.)

igure 9

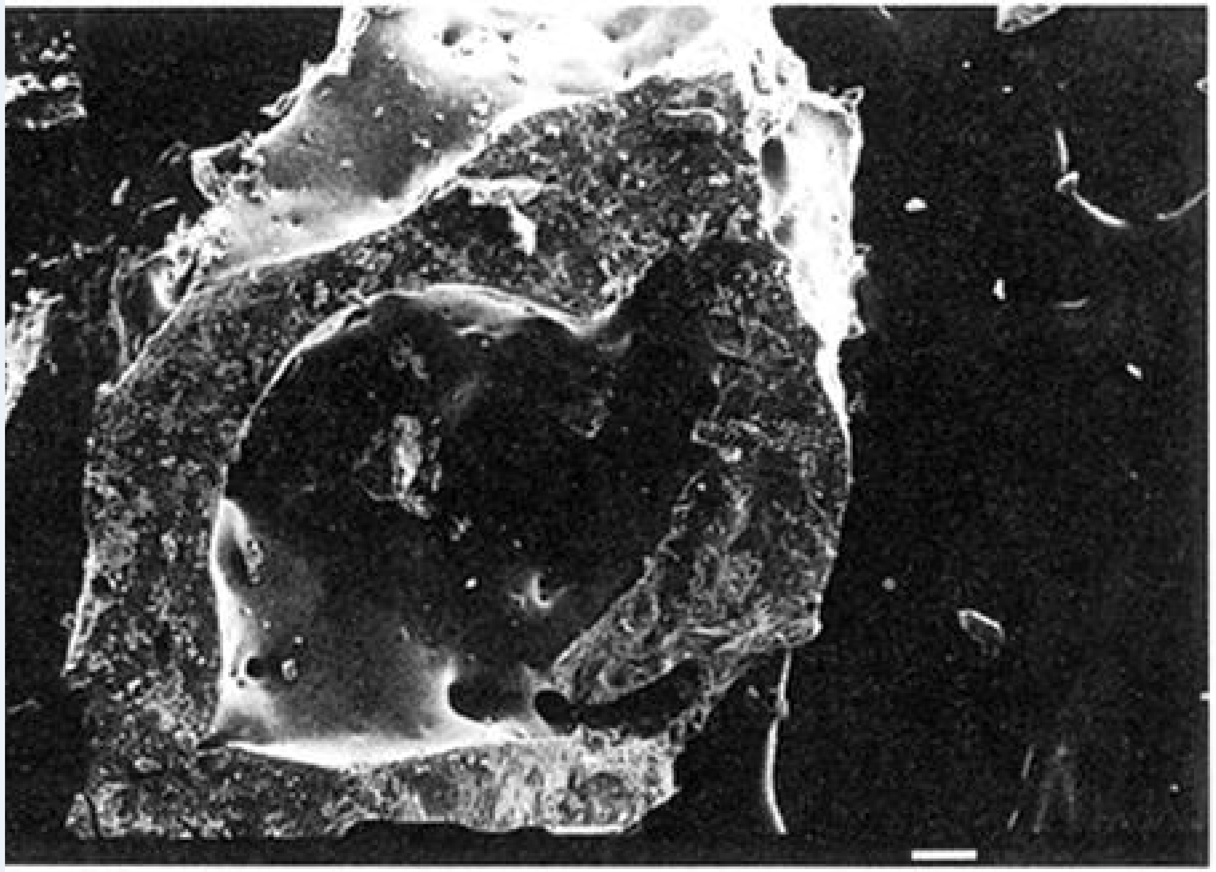

Figure 10

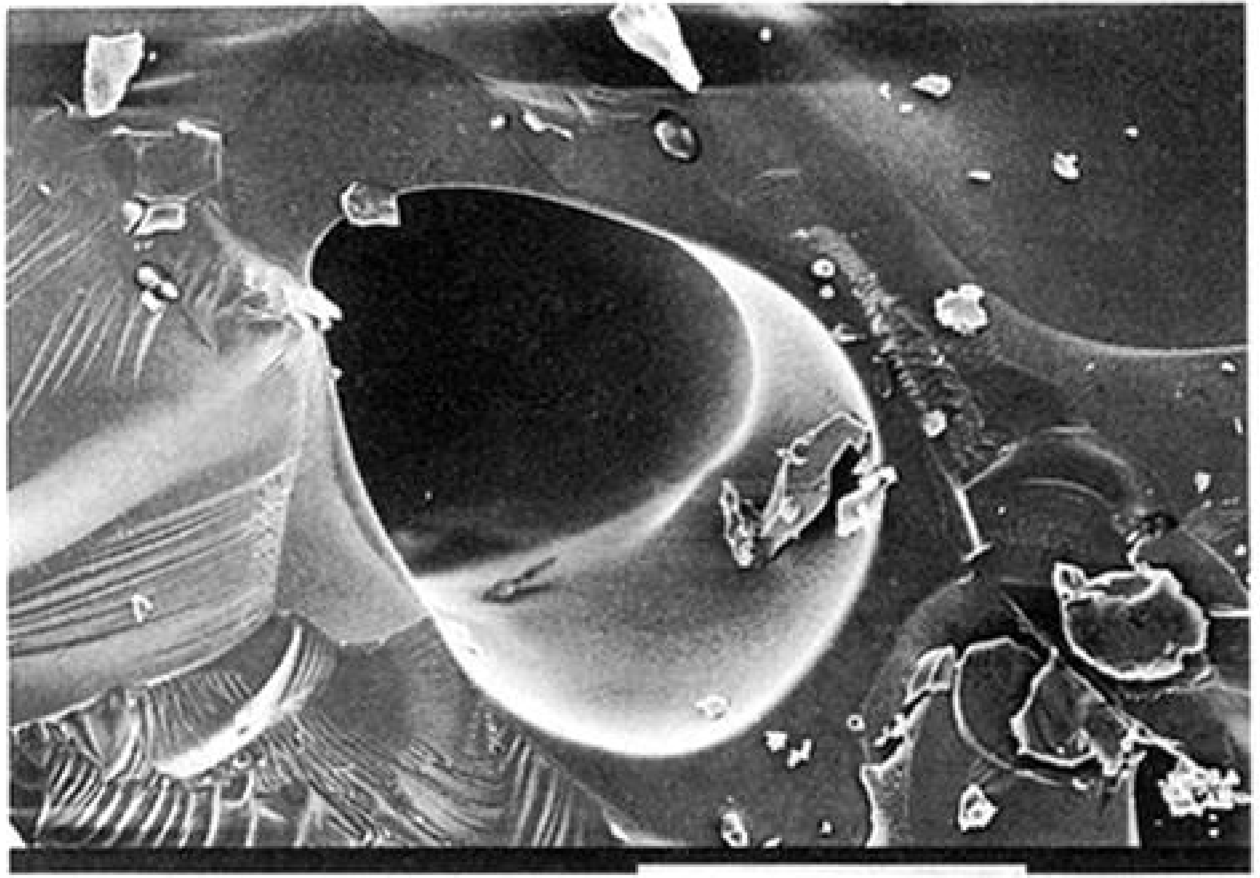

gure 9. This aggregate was formed by the fusion of crushed powder reactant at $\alpha = 0.1$ (430 K). racture of the sample revealed the large central hole. (Scale bar: 100 µm.)

gure 10. The cleavage surface of this aggregate formed by the sintering of a crushed powder mple ($\alpha = 0.60$ at 448 K) shows a large pore and coherent reactant phase in which no features or xtural variations can be discerned. (Scale bar: 100 µm.)

igure 11

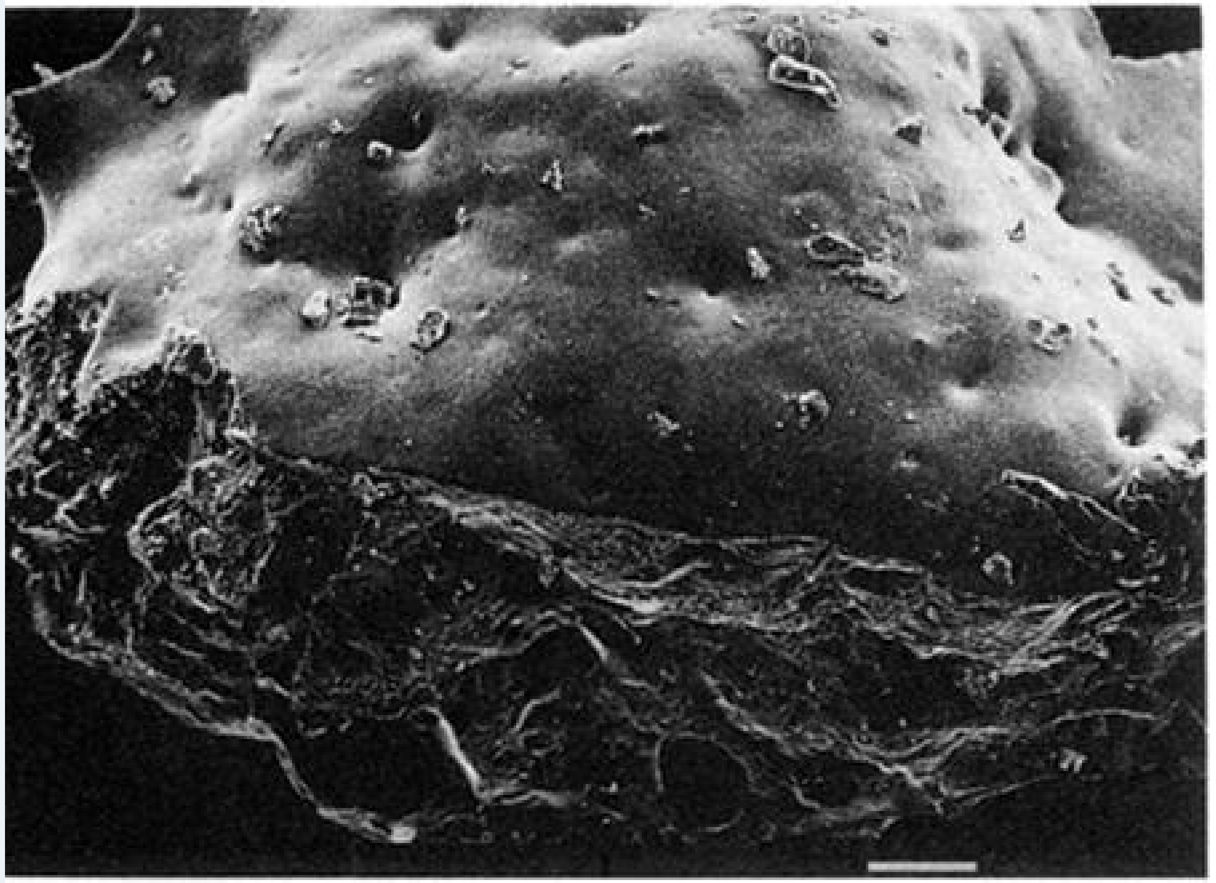

Figure 12

igure 11. At an early stage in dehydration of a crushed powder reactant sample ($\alpha = 0.1$ at 430 K) e fused salt showed superficial rounded features indicative of control by surface tension rather an crystallographic forces. (Scale bar: 100 μm.)

igure 12. On other surfaces of the same sample as figure 11 there were characteristic rounded rface features reminiscent of those (figure 2) identified as sites of bubble escape through a viscous uid medium. (Scale bar: 10 μm.)